Springer

Journal of Mechanical Science and Technology 23 (2009) 420~425

Journal of
Mechanical
Science and
Technology

www.springerlink.com/content/1738-494x
DOI 10.1007/s12206-008-1104-3

Fatigue characteristics of bearing steel in very high cycle fatigue †

Chang-Min, Suh[1] and Jong-Hyoung, Kim[2,*]

[1]*School of Mechanical Engineering, Kyungpook National University 1370, Sankyuk-Dong, Buk-gu, Daegu, 702-701, Korea*
[2]*Department of Mechanical Science and Engineering, Graduate School of Engineering, Nagoya University, Furo-cho, Chikusa-ku, Nagoya, Aichi 464-8603, Japan*

(Manuscript Received June 22, 2007; Revised September 4, 2008; Accepted October 31, 2008)

Abstract

Very high cycle fatigue (VHCF) tests were carried out to find the fatigue characteristics of a super-long life range by using a cantilever type rotational bending fatigue test machine on three kinds of specimens in bearing steel which were quenched and tempered in air (A: non-shot peened and B: shot peened after heat treatment) and under vacuum environment(C: non-shot peened) in this study. S-N curves obtained from the VHCF tests of the B and C specimens tend to come down again in the super-long life (10^9 cycles) range due to fish-eye type cracking, while most of the A and B specimens were fractured by surface defects such as scratches and slip lines. This duplex S-N behavior of bearing steel has to be reviewed by the change of the fracture modes.

Keywords: Very high cycle fatigue (VHCF); Rotational bending fatigue test; Shot peening; Fatigue characteristic; Fish-eye crack; Giga cycle fatigue

1. Introduction

According to recent industrial development, the VHCF behavior of materials in the super-long life range ($N>10^7$) has received attention with regard to safety in the design and reliability of machine elements [1-8]. Also, for many applications, the understanding of 10^9 (giga) cycle fatigue in materials becomes extremely important [10]. The fatigue behavior of structural materials in the very high cycle regime of 10^9~10^{10} cycles has become an important subject of research all over the world [9]. For high strength steels such as bearing steel, SNCM 439, SCM 435 and 0.46C steel were used for super-long life fatigue tests [1-4]. Some researchers reported that high strength steel and surface hardened steel indicated that the S-N curves obtained from the fatigue tests tended to come down again in the super-long life range due to fish-eye type internal cracking [1, 3, 14].

Others reported, however, a fish-eye crack (a typical fracture mode in the super-long life range over 10^6 cycles range) was not observed in all specimens and the crack initiation occurred on the surface of the SCN 435 specimen [5]. This duplex S-N behavior for high strength steel has to be reviewed by the change of the fracture modes.

In this study, bearing steel was quenched and tempered in air and under vacuum environment. VHC fatigue tests were conducted to obtain the characteristics of a super-long life range by using a cantilever type rotational bending fatigue test machine. The VHC fatigue fracture behavior in the super-long life was discussed based on the fractograph observation by a scanning electron microscope (SEM) and the residual stress was measured by an X-ray diffraction method.

2. Experimental procedure

2.1 Materials and specimens

The material used in this study was high carbon

† This paper was recommended for publication in revised form by Associate Editor Youngseog Lee
*Corresponding author. Tel.: +82 53 950 5573, Fax.: +82 53 950 6550
E-mail address: cmsuh@knu.ac.kr

Table 1. Chemical composition (wt %).

C	Si	Mn	P	S	Cu	Ni	Cr	Mo
1.04	0.25	0.39	0.015	0.005	0.19	0.07	1.47	0.004

Table 2. Mechanical properties.

Specimen	Heat Treatment	Shot peening	Tensile Strength (MPa)	Elongation (%)	Hardness (Hv)
A	In air	No	1735	3.55	710
B	In air	Yes			
C	In vacuum	No	1750	3.4	752

chromium steel (STB2, JIS material code: SUJ2) for the use of bearings. Table 1 shows the chemical compositions of the specimen tested in this experiment. The specimens after machining were put into heat treatment as follows: The specimens were heated at 1108K for 40 minutes and then quenched into 353K oil. Then the specimens were reheated to 453K for 40 minutes and cooled in air.

We classified the three kinds of specimens as follows:

A: Heat treated in air and non-shot peened specimen, $H_V \fallingdotseq 710$,
B: Heat treated in air and shot peened one, $H_V \fallingdotseq 710$,
C: Heat treated under vacuum with non-shot peened one, $H_V \fallingdotseq 752$.

Specimens for the VHC fatigue tests with round notch as shown in Fig. 2 were polished after these heat treatments. The notch radius is 7 mm and the stress concentration factor, K_t is 1.06. Specimens were polished to remove the decarburization layer after heat treatment by using abrasive paper up to #2000. After polishing, the specimens were buffed by chrome oxide (Cr_2O_3) to make a mirror surface. A shot peening process was applied to the specimens that were heat treated in air by using a shot-gun and cast steel balls. The diameter of the steel balls is about 0.6mm, and the peening pressure and time are about 0.83MPa and 3 minutes, respectively. Table 2 shows the mechanical properties of STB2 after heat treatment.

2.2 Fatigue test

The fatigue tester used in this study is a multi-cantilever type rotational bending fatigue machine

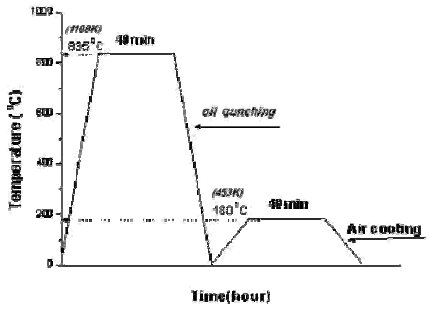

Fig. 1. Heat treatment process.

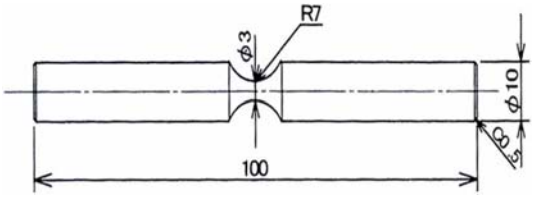

Fig. 2. Configuration of VHC fatigue specimen (unit : mm).

developed by the Research Group for Statistical Aspects of Materials Strength headed by T. Sakai [1] and manufactured by Horkos Co. (U00235). The tester has two spindles driven by an electric motor via a flat belt at a rotating speed of 3,150rpm. Each spindle has test specimen grips at both ends, so that the tester can test four fatigue specimens simultaneously.

2.3 Analysis and measurement

All of the specimens were tested at various loading conditions until fatigue fracture occurred. After the fatigue test, the fractured surface of every specimen was observed and analyzed by an SEM/EDX (energy dispersive X-ray spectrometry) system to identify the origin of fatigue initiation and the chemical compositions of the inclusion. The residual stress of the axis direction was measured by using an XRD (X-Ray Diffract Meter, Rigaku, MJ200DE) in the case of shot peened specimens. Electro-polishing was used to reduce its diameter.

3. Results and discussion

3.1 The effect of surface roughness on VHC fatigue

Usually, material under repeated bending stress is very sensitive to surface roughness at a low stress level that has a long fatigue life. Table 3 shows the results of the average roughness (R_a) and maximum roughness (R_{max}) measured on the specimen surface

Table 3. Surface roughness of the fatigue specimens before and after shot peening.

Specimen	R_a(μm)	R_{max}(μm)
A, C: Non-shot peened	0.04	0.4
B: Shot peened	1.95	10.6

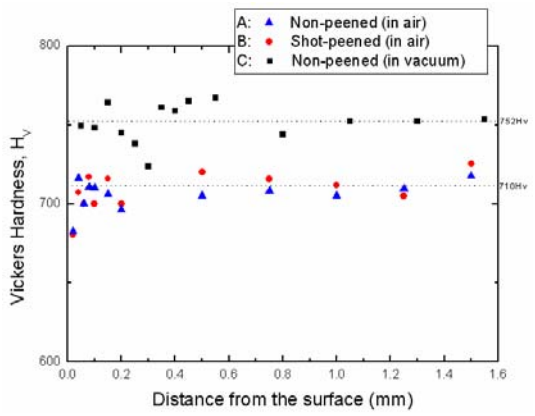

Fig. 3. Distribution of the micro Vickers hardness on the cross section.

in order to compare roughness changes before and after shot peening. From the table, it can be seen that the measured roughness R_{max} is about 10 times higher than that of R_a for the non-shot peened specimen (A and C) and about 5 times for the shot peened specimen (B). The measured roughness of a shot-peened specimen increased about 26 times higher than that of a non-shot peened one in the case of R_{max}. If there are no other effects, the increased surface roughness will affect the fatigue life of specimens which were tested at a low load level in a long life.

3.2 Hardness variation from the specimen surface

Fig. 3 shows the distribution of the micro-Vickers hardness on the cross section of the three kinds of specimen. The hardness profiles are fairly uniform from the surface to the center, and the average hardness values were estimated to be about $710H_V$ for both the A and B specimens. On the other hand, the C specimen had a value of 752 H_V. Moreover, it can be seen that the hardness of the A and B specimens close to the surface had their values decreased to about $680H_V$.

3.3 Residual stress on the specimen surface

From the test, the amount of residual stress measured by the X-ray diffraction method was -498MPa for the shot-peened specimen and -78MPa for the non-shot peened specimen. Both of the specimens had compressive residual stress on the surface. The compressive residual stress of the shot-peened specimen, however, increased 6.4 times higher than the non-shot peened one. Accordingly, it can be expected that the VHC fatigue life of the shot-peened specimen will be better than that of the non-shot peened one because the compressive residual stress that occurred by shot-peening will retard the crack initiation on the specimen.

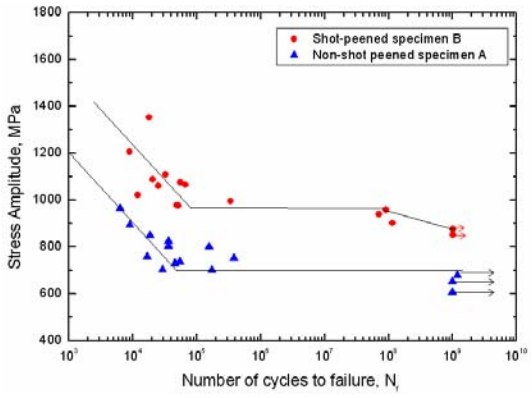

Fig. 4. The S-N curves for non-shot peened and shot peened specimens which were heat treated in air.

3.4 S-N diagram

Fatigue tests were performed to verify the fatigue characteristic of a giga cycle (10^9 cycles) about each specimen. Fig. 4 shows the S-N curves of the A and B specimens for quenched and tempered bearing steel in air. From the figure, the solid triangular symbol indicates fatigue life at the tested stress level for the non-shot peened A specimen, which does not show the duplex behavior of the S-N curves until the 10^9 cycles range. In these tests, most of the specimens were fractured by surface defects such as scratches and slip lines.

Solid circular symbols in Fig. 4, however, indicate the S-N curve of the shot peened B specimen, which shows the duplex behavior of S-N curves. Most of the specimens fractured by the cracks initiated from the surface defects were formed due to shot peening. The plotted data are scattered widely at each stress level. The two inclined lines show a duplex S-N diagram in the case of the shot peened specimen. The main factor which increases fatigue strength and life is dependent

upon the compressive residual stress formed on the surface by shot peening. The fatigue life of the shot peened B specimen increased about 36% more than that of the non-shot peened one at the 10^6 cycles range and increased about 26% at 10^9 cycle range.

Fig. 5 shows the S-N curves of the C specimen that was heat treated under vacuum environment. In these tests, most of the specimens tested at high stress levels and that had a short fatigue life less than 5x 10^5 cycles range, were fractured by cracks which initiated from surface defects such as scratches and slip lines and are marked as squared solid symbols in Fig. 5. On the other hand, specimens tested at low stress levels and that had a long fatigue life of more than 5x10^5 cycles range, were fractured due to fish-eye type cracks initiated at the subsurface inclusion and are marked as solid circular symbols in Fig. 5. Although the plotted data are scattered at each stress level, these results are similar to those of other researchers [1, 3]. Most of the surface fracture modes are plotted in the short fatigue life, while most of the fish-eye fracture modes belong to the long fatigue life (VHCF) range. In this figure, the solid squared symbols drop again over the 10^7 cycles range although obtained data are not enough to date. Duplex S-N curves similar to those in Fig. 5 have been reported by other researchers [1, 3].

In comparing the S-N curves in Fig. 5 with those in Fig. 4, it can be seen that decarburization which occurred by the heat treatment process in the air environment influences greatly the fatigue limit and fatigue life. The fatigue life of the non-shot peened C specimen increased about 86% more than that of the non-shot peened A specimen at the 10^6 cycles range and increased about 57% at 10^9 cycles range.

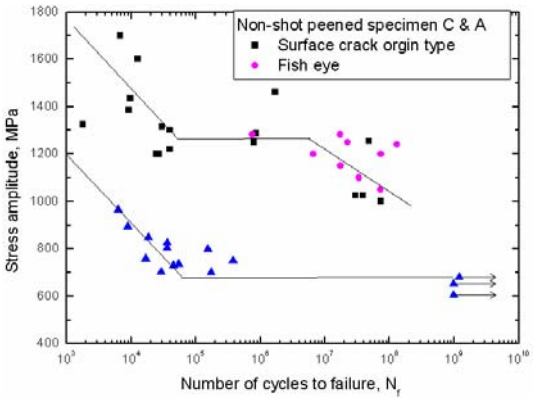

Fig. 5. The S-N curves for non-shot peened specimens which were heat treated under vacuum and in air.

3.5 Fatigue fractured pattern

From the SEM observation on the fatigue fractured surface, we classified two kinds of fracture modes. A major fatigue crack which leads to the final fracture of the specimen is initiated on the specimen surface, but no significant defect can be observed at the crack origin. On the other hand, inclusions near the surface or subsurface can make a fish-eye crack lead to a fatigue fracture.

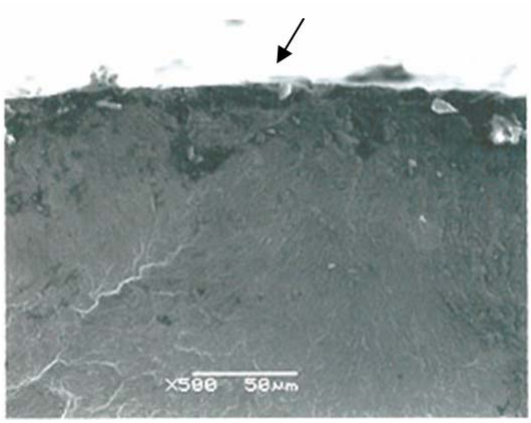

Fig. 6. SEM photograph of fracture surface for shot-peened B specimens under σ_a=957MPa, N_f = 9.12×10^8 cycles (×500). An arrow indicates the origin of the surface crack initiation site.

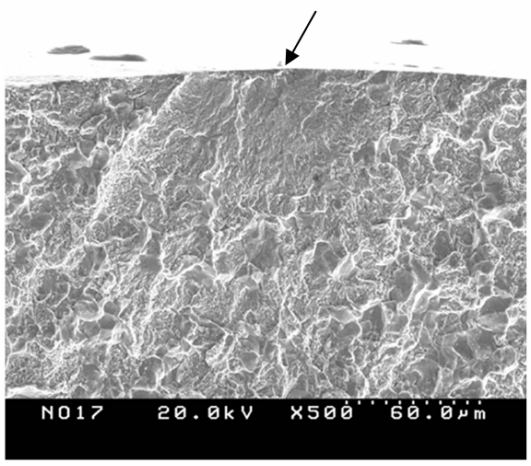

Fig. 7. SEM photograph of fracture surface for C specimen under σ_a=1,600MPa, N_f = 1.26×10^4 cycles (×500). An arrow indicates the origin of the surface crack initiation site.

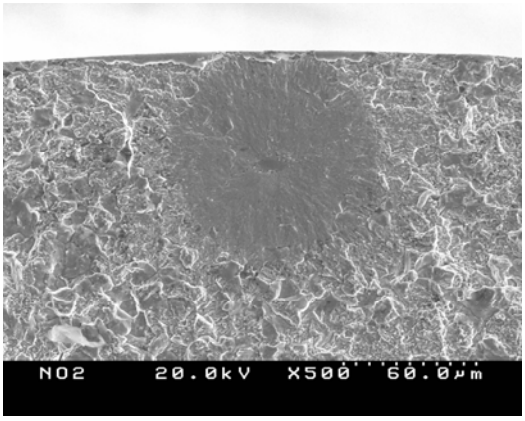

Fig. 8. SEM photograph of fracture surface for C specimen under σ_a = 1,282MPa, $N_f = 7.54\times10^5$ cycles (×500).

Fig. 6 shows an example of a fatigue-fractured surface for shot peened B specimen under σa= 957MPa, Nf = 9.12×10^8 cycles at a magnification of ×500 and displays VHC fatigue initiation of a surface crack origin type (surface crack style).

Fig. 7 shows an example of a fatigue-fractured surface for C specimen tested at σ_a= 1,600MPa, $N_f = 1.26\times10^4$ cycles. The initial crack that leads to final fatigue fracture is caused by the surface crack origin type.

Fig. 8 shows an example of a fish-eye crack fractured surface for C specimen tested at σ_a= 1,282MPa, $N_f = 7.54\times10^5$ cycles. The initial crack that leads to final fatigue fracture is affected by a fish-eye crack from a chromium oxide inclusion. This pattern was observed by many researchers [1, 3-6].

Fig. 9 shows the relationship between the radius of fish-eye crack a or b and its depth d. In this figure, we plotted the Nakasone data [3] for comparison. The radii a and b of fish-eye are almost equal to both data and also to its diameter. This figure implies that a fish-eye crack can grow larger for a deeper depth of a inclusion and the same behavior was obtained in the Nakasone et al. report [3].

3.6 EDX analysis of inclusions on fracture surface

An EDX spectrum was obtained from the center of an inclusion of Fig. 8. Iron Fe is the main compositional element with a weight % of 59.6 and a chromium oxide (Cr_2O_3) compose with a weight % of 40.4.

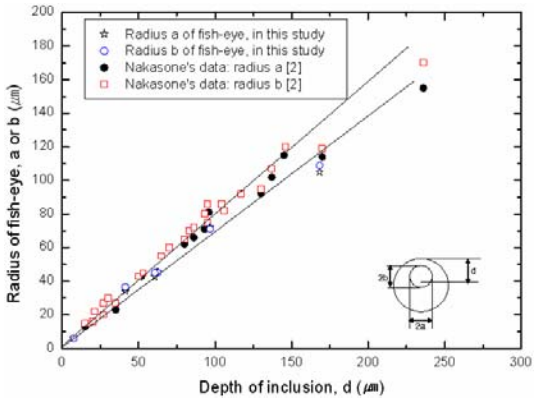

Fig. 9. Relationship between fish-eye radius and its depth of inclusion.

4. Conclusions

The main results obtained in this study are as follows:

(1) The duplex S-N curves were obtained from B and C specimens for bearing steel, and confirmed two kinds of fracture modes: a surface crack origin type in the case of shorter life region of $N_f < 5\times10^5$ cycles range and a fish-eye crack (internal crack origin) in the case of a longer life region of $N_f > 5\times10^5$ cycles range.

(2) The EDX analysis of an inclusion that initiated a fish-eye crack revealed that chromium oxide was the dominant compositional element in the center of it.

(3) Decarburization which occurred by a heat treatment process in the air environment has a great influence on the fatigue limit and fatigue life.

Acknowledgment

This work was supported by the Brain Korea 21 project.

References

[1] T. Sakai, M. Takeda, K. Shiozawa, Y. Ochi, M. Nakajima, T. Nakamura and N. Oguam, Experimental reconfirmation of characteristic S-N property for high cabon chromium bearing steel in wide life region in rotating bending, J. Soc. Mat. Sci., Japan, 49 (2000) 779-785.

[2] K. Shiozawa, Y. Morii and S. Nishino, Subsurface crack initiation and propagation mechanism under the super-long fatigue regime for high speed tool

steel (JIS SKH51) by fracture surface topographic analysis" JSME International Journal Series A, 49 (1) (2006) 1-10.

[3] Yuji. Nakasone and Hiroaki. Hara, FEM simulation of growth of fish-eye cracks in the very high cycle fatigue of a high strength steel SUJ2 Pro. of 3rd Int. Conf. on Very High Cycle Fatigue (VHCF-3) (2004), 40-47.

[4] T. Sakai, Crack initiation mechanism of bearing steel in high cycle fatigue, Fracture of Nano and Engineering Material and Structure, (2006), 1129-1130.

[5] Q. Y. Wang, Y. Berard, A. Dubarre, G. Baudry, S. Rathery and C. Bathias, Giga cycle fatigue of ferrous alloys, Fatigue Fract. Engng. Mater. Struc. 22 (1999) 667-672.

[6] Y. Murakami, T. Nomoto and T. Ueda, Factors influencing the mechanism of superlong fatigue in steel, Fatigue Fract. Engng. Mater. Struct., 22(1999), 581-590.

[7] S. Nishijima and K. Kanazawa, Stepwise S-N curve and fish-eye failure in giga cycle fatigue, Fatigue Fract. Engng. Mater. Struct., 22(1999), 601-607.

[8] Q. Y. Wang, C. Bathias, N. Kawagoishi and Q. Chen, Effect of inclusion on subsurface crack initiation and giga cycle fatigue strength" Int. J. of Fatigue, 24(2002), 1269-1274.

[9] Tatsuo Sakai, Importance of standardization for fatigue testing and fatigue data analysis in very high cycle regime, Experimental Analysis of Nano and Engineering Material and Structure, (2007), 243-244.

[10] Q. Y. Wang, H. Zhang, M. R. Sriraman and S. X. Li, Very long life fatigue behavior of bearing steel AISI 52100 Key Engineering Materials 297-300 (2005) 1846-1851.

[11] Murakami, Takada and Toriyama, Super-long life tension-compression fatigue properties of quenched and tempered 0.46% carbon steel, Int. J. Fatigue 16, 9(1998),.661-667.

[12] Jong-Gyu Lee and Jung-Kyu Kim, Influence of residual stress due to shot peening on fatigue strength and life, KSME International Journal (A), 21-9(1997), 1498-1506.

[13] Chang-Min Suh, Byung-Won Hwang and Murakami, Characteristic of fatigue crack initiation and fatigue strength of nitride 1Cr-1Mo-0.25V turbine rotor steels, KSME International Journal, 16 (8) (2002) 1109-1116.

[14] Israel Marines-Garcia, Paul C. Paris, Hiroshi Tada and Claude Bathias, Fatigue crack growth from small to long cracks in VHCF with surface initiations, International Journal of Fatigue 29(2007), 2072-2078.

Chang-Min Suh received his B.S. and M.S. degrees in mechanical engineering from Busan Na-tional University in 1964 and 1968, respectively, and received his Ph.D. degree from the University of Tokyo in 1981. He now is a professor at Kyungpook National University. He has served as the Head of the Department of Mechanical Engineering at Kyungpook National University, a Visiting Professor of Materials Science and Engineering in Univ. of California Berkeley, a Head of the Institute of Engineering Design Technology Kyungpook Nat'l Univ, and a Head of the Technology Innovation Center designated by the Department of Commerce and Industry of Korea.